Downloaded from rsta.royalsocietypublishing.org

PHILOSOPHICAL TRANSACTIONS OF THE ROYAL SOCIETY A MATHEMATICAL, PHYSICAL & ENGINEERING SCIENCES

Leakage Currents in a Segmented Electrode Generator

M. G. Haines

Phil. Trans. R. Soc. Lond. A 1967 **261**, 440-454
doi: 10.1098/rsta.1967.0012

Email alerting service

Receive free email alerts when new articles cite this article - sign up in the box at the top right-hand corner of the article or click **here**

To subscribe to *Phil. Trans. R. Soc. Lond. A* go to: **http://rsta.royalsocietypublishing.org/subscriptions**

This journal is © 1967 The Royal Society

Downloaded from rsta.royalsocietypublishing.org

VIII. Leakage currents in a segmented electrode generator

By M. G. Haines

Physics Department, Imperial College, London, S.W. 7; and consultant to International Research and Development Co. Ltd, Newcastle upon Tyne 6

Segmented electrodes are being used extensively in magnetohydrodynamic flow experiments in order to overcome the high impedance present in a continuous electrode system when the plasma has a high Hall coefficient. Until recently the theoretical study of a segmented system has artificially constrained the current to flow directly across the duct. Since this present work was undertaken Witalis has investigated the onset of shorting of the Hall voltage between adjacent segments by leakage currents due to insufficiently long insulator sections, by assuming that the segmentation length is much smaller than the duct width. In this paper three methods are adopted for analysing the effect of leakage currents and obtaining the electrical characteristics. These are conformal mapping, Fourier series and an approximate equivalent circuit. Only the Fourier analysis method requires no further assumptions other than periodicity and it reproduces Witalis's criterion for shorting when his additional assumptions apply. The equivalent circuit method is easier to apply and will be more useful for a practical non-uniform duct.

Introduction

The plasmas that are commonly used in magnetohydrodynamic power generation experiments possess a high Hall parameter β ($\simeq eB/\eta_a e_{ea}$ from equations (10) and (11)). This is because large magnetic fields are employed to obtain maximum interaction per unit volume and because, being only slightly ionized, the dominant electron–atom collision cross-section which determines the resistivity is small. Under these conditions β is independent of electron density. The Hall effect can be included implicitly in a tensor conductivity or written explicitly in an Ohm law containing a scalar conductivity. It is easier here to adopt the latter method.

The principal feature of the Hall effect is that the current flows at an angle $\theta = \tan^{-1}\beta$ to the total Lorentz electric field. In a rectangular m.h.d. duct with continuous highly conducting electrodes, the Lorentz electric field is perpendicular both to the direction of plasma flow (which is parallel to the electrode surfaces) and to the magnetic field. The current flows across the channel at the Hall angle, i.e. there is a component parallel to the flow. This has two disadvantages. It causes the braking magnetomotive force to be at the Hall angle to the plasma flow and also increases the internal impedance of the generator. By segmenting the electrodes, an electric field component parallel to the electrode surface and antiparallel to the plasma flow can be developed which, under idealized conditions, tilts the total Lorentz electric field vector backwards at the Hall angle so that the current flows directly across the duct. This is the ideal mode of operation of a Faraday generator.

It is easily seen that the length of each segment must be much smaller than the width of the duct in order to be effective in constraining the current to flow directly across the duct. What is not so obvious is the optimising ratio of insulator length to electrode length in each segment. A large ratio would cause a high internal impedance near the electrode

The Royal Society is collaborating with JSTOR to digitize, preserve, and extend access to *Philosophical Transactions of the Royal Society of London. Series A, Mathematical and Physical Sciences.* www.jstor.org

Downloaded from rsta.royalsocietypublishing.org

owing to the high concentration of current there. However, because the electric field is normal to the electrode surface, the current enters the electrode at the Hall angle to the normal and tends to concentrate on one electrode end. Therefore a smaller ratio does not reduce the impedance substantially. At small ratios of the insulator to electrode length current leakage will occur across adjacent segments thus making the segmentation less effective. Near the insulator surface, since there is no current or flow velocity normal to the surface, the electric field E_x along the direction of plasma flow is equal to j_x/σ. Hence it can be seen that if E_x does not change sign along the path joining adjacent electrodes then current shorting or leakage will occur.

The purpose of this paper is to examine this shorting mechanism which has so far been neglected. Crown (1961) pointed out the mechanism qualitatively. Since the author undertook this work, however, Witalis (1965) has published an analysis of a segmented generator including the shorting effect. The notation here is adapted to that of Witalis. Three methods of solution are put forward here, namely a conformal transformation (as used also by Witalis), a Fourier analysis and an approximate equivalent electrical circuit.

Physical model and assumptions

The basic equations used are the Maxwell equations and the Ohm law. For a slightly ionized gas Schluter (1950, 1951) and Kemp & Petschek (1958) have derived an appropriate Ohm law. Taking the basic conditions for very slight ionization and electrical neutrality, namely

$$n_a \gg Zn_i = n_e, \tag{1}$$

the following ordering procedure eliminates the dynamical terms in the electron and ion momentum equations, where $m_i \sim m_a \gg m_e$:

$$\mathbf{E} \sim \mathbf{v}_i \times \mathbf{B} \sim \mathbf{v}_e \times \mathbf{B} \sim \frac{\boldsymbol{j} \times \mathbf{B}}{n_e e} \sim \frac{\nabla P_a}{n_e e} \sim \frac{n_a m_a}{n_e e} \frac{\mathrm{d}\mathbf{v}_a}{\mathrm{d}t} \gg \frac{m_i}{e} \frac{\mathrm{d}\mathbf{v}_i}{\mathrm{d}t} \sim \frac{\nabla P_i}{n_i e} \sim \frac{\nabla P_e}{n_e e} \gg \frac{m_e}{e} \frac{\mathrm{d}\mathbf{v}_e}{\mathrm{d}t}.$$

This is valid provided there are no sharp discontinuities in the magnetic field. Then writing frictional forces proportional to the difference in the mean velocity of the components, the three momentum equations become

$$0 = Zen_i(\mathbf{E}+\mathbf{v}_i \times \mathbf{B}) + n_i n_e \epsilon_{ie}(\mathbf{v}_e - \mathbf{v}_i) + n_i n_a \epsilon_{ia}(\mathbf{v}_a - \mathbf{v}_i), \tag{2}$$

$$0 = -en_e(\mathbf{E}+\mathbf{v}_e \times \mathbf{B}) + n_i n_e \epsilon_{ie}(\mathbf{v}_i - \mathbf{v}_e) + n_e n_a \epsilon_{ea}(\mathbf{v}_a - \mathbf{v}_e), \tag{3}$$

$$n_a m_a \, \mathrm{d}\mathbf{v}_a/\mathrm{d}t + \nabla P_a = n_i n_a \epsilon_{ia}(\mathbf{v}_i - \mathbf{v}_a) + n_e n_a \epsilon_{ea}(\mathbf{v}_e - \mathbf{v}_a), \tag{4}$$

where

$$\epsilon_{jk} = \frac{8}{3}\sqrt{\left(\frac{2kT}{\pi}\frac{m_j m_k}{m_j + m_k}\right)} Q_{jk}$$

and Q_{jk} is the elastic collision cross section. Consistent with the ordering procedure the total density ρ and centre of mass velocity $\mathbf{v}$ are $n_a m_a$ and $\mathbf{v}_a$ respectively. Defining an ion slip velocity $\mathbf{v}_s = \mathbf{v}_a - \mathbf{v}_i$ and electric current density $\boldsymbol{j} = n_e e(\mathbf{v}_i - \mathbf{v}_e)$ equations (2) to (4) give

$$\rho \mathrm{d}\mathbf{v}/\mathrm{d}t + \nabla p = \boldsymbol{j} \times \mathbf{B}, \tag{5}$$

$$\mathbf{v}_s(Z^{-1}\epsilon_{ia} + \epsilon_{ea}) n_e n_a = -\boldsymbol{j} \times B - \boldsymbol{j} n_a \epsilon_{ea}/e, \tag{6}$$

and

$$\mathbf{E} + \mathbf{v} \times \mathbf{B} - \frac{\boldsymbol{j} \times \mathbf{B}}{n_e e}\left[\frac{Z^{-1}\epsilon_{ia} - \epsilon_{ea}}{Z^{-1}\epsilon_{ia} + \epsilon_{ea}}\right] + \frac{(\boldsymbol{j} \times \mathbf{B}) \times \mathbf{B}}{n_e n_a (Z^{-1}\epsilon_{ia} + \epsilon_{ea})} = \frac{\boldsymbol{j}}{e^2}\left[\epsilon_{ei} + \frac{n_a}{n_e}\frac{Z^{-1}\epsilon_{ia}\epsilon_{ea}}{Z^{-1}\epsilon_{ia} + \epsilon_{ea}}\right]. \tag{7}$$

Downloaded from rsta.royalsocietypublishing.org

Equation (5) is the equation of motion, (6) relates the ion slip to the current density and (7) is the appropriate Ohm law. In (7) the first two terms are the Lorentz electric field, next we have the Hall electric field and then the characteristic ion slip term. In contrast to Kemp & Petschek $\mathbf{v}_s$ in (6) contains a term in j as well as $j \times \mathbf{B}$, and the ratio of the two terms is approximately the same as the corresponding terms in Ohm law (equation (7)). Thus neither can be neglected.

An insight into the mechanism which leads to the slowing down and extraction of power from neutral atoms can be obtained from these equations using

$$\epsilon_{ea}/\epsilon_{ia} \sim \sqrt{(m_e/m_i)} \ll 1.$$

In a segmented generator the electrons are braked by the Lorentz force acting on them as they carry the current across the duct. There is a space charge electric field set up—the Hall electric field—which decelerates the ions. The neutrals are slowed down by friction with the ion gas. If the generator is not segmented then no electric field parallel to the flow can exist. Then the ions rely on friction with the electrons to brake their motion. This frictional force is proportional to the excess velocity of ions over electrons in the direction of flow which constitutes a positive Hall current.

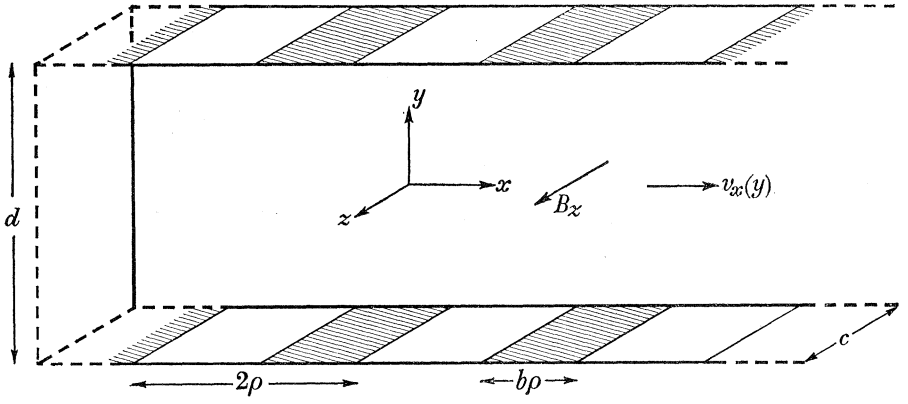

FIGURE 1. A sketch of a constant area segmented electrode duct section indicating the symbols used in the paper.

In Witalis's notation, the magnetohydrodynamic generator duct is illustrated in figure 1. Oppositely connected electrodes are separated by the duct width d, the dimension parallel to the magnetic field having a length c. A complete insulator and electrode have a length 2ρ and the insulator length is $b\rho (0 \leqslant b \leqslant 2)$. With $\mathbf{B} = (0, 0, B_z)$,

$$\mathbf{v} = (v_x(x, y), 0, 0), \quad j = (j_x(x, y), j_y(x, y), 0) \quad \text{and} \quad \mathbf{E} = (E_x(x, y), E_y(x, y), 0),$$

the Ohm law (equation (7)), can be written in the component form

$$j_x = \sigma E_x - \beta j_y, \tag{8}$$

$$j_y = \sigma(E_y - v_x B_z) + \beta j_x, \tag{9}$$

where

$$\beta = \frac{\sigma B}{n_e e} \frac{Z^{-1}\epsilon_{ia} - \epsilon_{ea}}{Z^{-1}\epsilon_{ia} + \epsilon_{ea}} = \tan\theta, \tag{10}$$

and

$$\frac{1}{\sigma} = \frac{1}{e^2}\left[\epsilon_{ei} + \frac{n_a}{n_e}\frac{Z^{-1}\epsilon_{ia}\epsilon_{ea}}{Z^{-1}\epsilon_{ia} + \epsilon_{ea}}\left(1 + \frac{e^2 B^2}{n_a^2 \epsilon_{ia}\epsilon_{ea}}\right)\right]; \tag{11}$$

θ, β and σ are the reduced Hall angle, Hall parameter and conductivity respectively.

Downloaded from rsta.royalsocietypublishing.org

In steady state, Maxwell's equations give

$$\operatorname{div} \boldsymbol{j} = 0 = \frac{\partial j_x}{\partial x} + \frac{\partial j_y}{\partial y}, \tag{12}$$

$$\operatorname{curl}_z \mathbf{E} = 0 = \frac{\partial E_y}{\partial x} - \frac{\partial E_x}{\partial y}. \tag{13}$$

With the aid of (12) and (13) the operation $\partial(8)/\partial y - \partial(9)/\partial x$ yields

$$\frac{\partial j_x}{\partial y} - \frac{\partial j_y}{\partial x} = \sigma\left[\frac{\partial E_x}{\partial y} - \frac{\partial E_y}{\partial x}\right] - \beta\left[\frac{\partial j_x}{\partial x} + \frac{\partial j_y}{\partial y}\right]$$

$$= \operatorname{curl}_z \boldsymbol{j} = 0. \tag{14}$$

Therefore $\boldsymbol{j}$ can be represented as the gradient of a scalar function ψ satisfying Laplace's equation

$$\boldsymbol{j} = -\nabla\psi, \tag{15}$$

$$\nabla^2\psi = \frac{\partial^2\psi}{\partial x^2} + \frac{\partial^2\psi}{\partial y^2} = 0. \tag{16}$$

In addition, writing $\mathbf{E}' = \mathbf{E} + \mathbf{v} + \mathbf{B}$ we see below that the angle θ between the current density vector and the Lorentz electric field vector is a constant, namely $\tan^{-1}\beta$. Also $\mathbf{E}' \times \boldsymbol{j}$ is in the direction of the magnetic field $\mathbf{B}_z$; hence

$$\hat{z}\tan\theta = \frac{\mathbf{E}' \times \boldsymbol{j}}{\mathbf{E}' . \boldsymbol{j}} = \hat{z}\beta.$$

Therefore, with $\mathbf{E}'_x = \mathbf{E}_x = 0$ near the surface of the highly conducting electrode, the current is emitted at an angle θ to the normal. Similarly, near the surface of the insulator, $j_y = 0$ implies that $\mathbf{E}'$ is at an angle θ to the surface.

Method I. Conformal transformation

Because, in this simplified model, the problem has been reduced to a two-dimensional solution of Laplace's equation the method of conformal transformation can be used. Writing $z = x + iy$ it can be noted that in the z plane the boundaries of the duct are straight but the current density pattern is in general very non-uniform with large concentrations at electrode edges and even current reversal if shorting between adjacent electrode segments occurs. The purpose of transforming to another plane is to straighten out the current density flux lines and the Lorentz electric field lines to a uniform mesh at an angle θ. This is carried out at the expense of distorting considerably the xy coordinates in this new $w = u + iv$ plane. However, if the original boundary conditions for ψ are known then the new boundaries of the duct in the w plane can be found. The appropriate boundary conditions can be found from a careful study of figure 2.

In figure 2 (a) is sketched the current flow between oppositely connected segment pairs in the absence of Hall effect, i.e. $\beta = 0$. In this symmetrical situation E_x and j_x will reverse in sign midway along the insulator, i.e. there is a stationary point of ψ here. For small β (figure 2 (b)) this stationary point shifts towards one electrode, indicating a net potential difference between adjacent segments. For larger values of the Hall parameter, or smaller insulator length $b\rho$, this stationary point (located in Witalis's notation at $a\rho$) can be moved to the electrode. This means that a shorting current j_x is now able to flow from

PHILOSOPHICAL TRANSACTIONS OF THE ROYAL SOCIETY A MATHEMATICAL, PHYSICAL & ENGINEERING SCIENCES
PHILOSOPHICAL TRANSACTIONS OF THE ROYAL SOCIETY A MATHEMATICAL, PHYSICAL & ENGINEERING SCIENCES

Downloaded from rsta.royalsocietypublishing.org

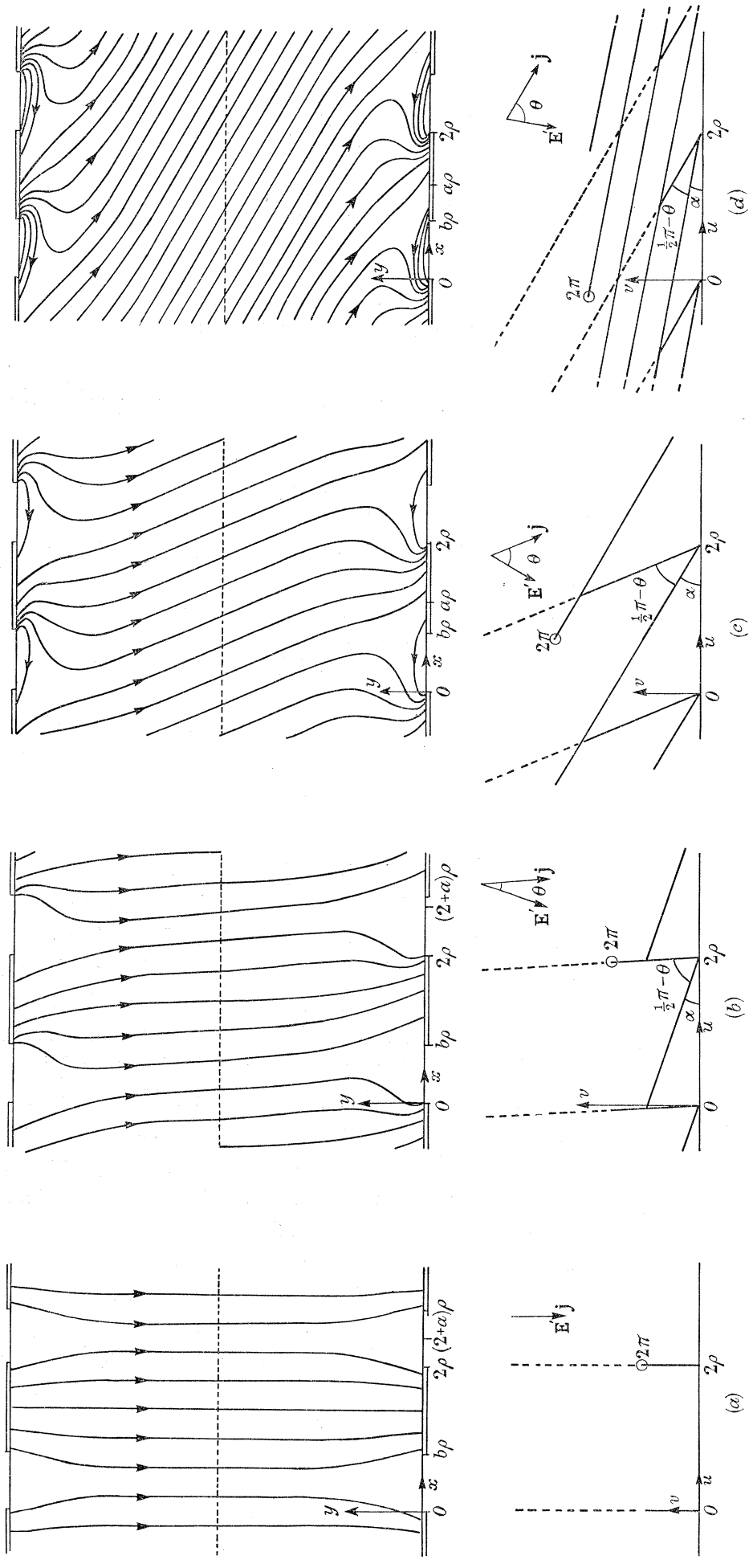

FIGURE 2. A sketch of current distributions between segmented electrodes and the corresponding conformal mapping of the lower duct wall (*a*) in absence of Hall effect, (*b*) for Hall effect present but no shorting, (*c*) with shorting between adjacent segments, (*d*) with extreme shorting.

PHILOSOPHICAL TRANSACTIONS OF THE ROYAL SOCIETY A MATHEMATICAL, PHYSICAL & ENGINEERING SCIENCES

PHILOSOPHICAL TRANSACTIONS OF THE ROYAL SOCIETY A MATHEMATICAL, PHYSICAL & ENGINEERING SCIENCES

Downloaded from rsta.royalsocietypublishing.org

one electrode to an adjacent one close to the insulator wall. This is illustrated in figure 2 (*c*). Figure 2 (*d*) pictures a more drastic condition when no current flows directly across the duct between oppositely connected electrodes. Then segmentation is not very effective, and this is the case for small b.

An exact transformation of the segmented duct to the w plane is difficult. This is because the complete electrode section should be specified in order to complete the boundary conditions around a closed path. The path in this case is a polygon and an intermediate Schwarz–Cristoffel transformation to a ζ plane is required to bring all the branch points and poles on to the real axis. Then the upper half plane of the ζ plane is transformed to the inside of a polygon which, for an n segment pair electrode system, will possess $6n-2$ sides.

Two approximate techniques have been used to simplify the problem. Hurwitz, Kilb & Sutton (1961) in a classic paper assumed that the duct was infinitely long and that the current distribution was periodic in the x direction with a periodic length 2ρ. They assumed that the duct width was large compared to the segmentation length, i.e. $d/2\rho \gg 1$, and that the current was homogenous in the centre of the duct. Only the case $b = 1$ (equal electrode and insulator lengths) was considered, and under these assumptions they showed that this will not lead to shorting of adjacent electrodes, i.e. $a \leqslant 1$ always. Recently Witalis (1965) has extended this work for any value of b and his work which includes the shorting mode duplicates much of the work carried out by the present author.

The second approximate technique has been developed by Schultz-Grunow & Denzel (1964) and does not use the assumption $d/2\rho \gg 1$. Instead straight lines are drawn across the duct from one insulator to an opposite insulator and it is assumed that no current flows across these lines. The problem is then reduced to a two-electrode configuration, but this artificial restriction prevents the consideration of leakage currents, and cannot represent the generator duct in the limit of small b.

The condition for the onset of shorting can be obtained by the transformation of Witalis. Only one boundary is transformed and the centre of the duct is assumed to be very far away. If we choose this boundary to be the real x axis no intermediate transformation is required. The transformation is illustrated in figure 2. At the stationary point $a\rho$, $\mathbf{j}$ and $\mathbf{E}'$ go through an angle π while at the start of the electrode, $x = b\rho$, the change is $-(\frac{1}{2}\pi - \theta)$ and at the end of the electrode, $x = 2\rho$, the change is $-(\frac{1}{2}\pi + \theta)$. Since this occurs with periodicity $2n\rho$ with a zero net change of angle, the upper half of the z plane is transformed into the upper part of the w plane bounded by an unclosed polygon using the following Schwarz–Cristoffel transformation and the Wierstrass product expansion.

$$\frac{\mathrm{d}w}{\mathrm{d}z} = k \prod_{n=-\infty}^{\infty} \frac{z + a\rho - 2n\rho}{(z - b\rho + 2n\rho)^{\frac{1}{2}-\theta/\pi}(z + 2n\rho)^{\frac{1}{2}+\theta/\pi}}$$

$$= k \frac{\sin \frac{1}{2}\pi(z/\rho - a)}{[\sin \frac{1}{2}\pi(z/\rho - b)]^{\frac{1}{2}-\theta/\pi}[\sin \frac{1}{2}\pi(z/\rho)]^{\frac{1}{2}+\theta/\pi}}. \tag{17}$$

The scale of the w plane is chosen such that

$$\lim_{y\to\infty} \left| \frac{\mathrm{d}w}{\mathrm{d}z} \right| = 1, \tag{18}$$

and the orientation similarly as

$$\lim_{y\to\infty} \left(\arg \frac{\mathrm{d}w}{\mathrm{d}z} \right) = 0. \tag{19}$$

Downloaded from rsta.royalsocietypublishing.org

Then $k = e^{-i\alpha}$ where the current flows at an angle $(\theta-\alpha)$ to the y direction. Equation (19) then yields an equation relating a and α

$$a-b(\tfrac{1}{2}-\theta/\pi)-2\alpha/\pi = 0. \tag{20}$$

Following Witalis, we can simplify the transformation to a pure translation as $y \to \infty$

$$\lim_{y\to\infty}(w-z) = \int_0^\infty \left(\frac{dw}{dz}-1\right)_{z=iy} dz = \rho\Delta_u + i\rho\Delta_v, \tag{21}$$

where the shifts Δ_u and Δ_v are functions of b, θ and α, given by Witalis and derived in several forms in the appendix.

The angle α can be determined by prescribing the external connexion of electrodes. If externally connected electrodes are placed geometrically opposite each other, then in the w plane they are staggered because the current flows at an angle $(\theta-\alpha)$ to the v axis. If we envisage a transform of the complete duct, the insulators on opposite sides of the duct are, in the transformed w plane, collinear, this common line being the current dividing line in the w plane between adjacent electrode pairs. The line $x = \frac{1}{2}b\rho$ transforms into the w plane as a (curved) line which, by symmetry, intersects the current dividing line in the middle of the duct corresponding to $y = \frac{1}{2}d$ in the z plane. Hence, for $d/2\rho \gg 1$,

$$\tan(\theta-\alpha) = -\frac{[u]}{[v]} = -\frac{\frac{1}{2}b\rho+\rho\Delta_u}{\frac{1}{2}d+\rho\Delta_v}. \tag{22}$$

From equations (20) and (22), a and α can be determined for a given b and d. $(\Delta_u+\frac{1}{2}b)$ is generally negative. Witalis has shown that oppositely connected electrodes, as given by equation (22), yields a maximum efficiency.

The conformal mapping of the lower electrode–insulator section is illustrated for the four examples in figure 2 discussed above. A change of π in the direction of the current density or electric field in the z plane results in a change of 2π in the w plane. Therefore at the positions $x = a\rho+2n\rho$ 'fins' are developed in the w plane as in a similar problem of a four-electrode germanium gyrator solved by Wick (1954). In figure 2 (a) and (b) where no current leakage occurs ($a < b$) the fins in the w plane protrude in the direction of j showing that no current is normal to their surface (the fins of course are part of the insulating surface) but the fins do indicate a reversal of $\mathbf{E}'$, i.e. there is a potential maximum at the tip. In figure 2 (c) and (d) where current shorting occurs ($a > b$) the fins are part of the transformed electrode surface and protrude in a direction perpendicular to $\mathbf{E}'$, such that, on any one electrode, some current is received from the adjacent electrode downstream, some comes from the other side of the duct—not necessarily from the geometrically opposite electrode—and some is lost (behind the fin) to the adjacent electrode upstream. If external loads are connected only across geometrically opposite electrodes, then, across any path connecting oppositely placed insulators there is no net current. Thus the backstream leakage currents near the insulator walls are compensated by a forward 'Hall' current in the central region of the duct.

It can be seen from figure 2 (d) that as the insulator thickness becomes very small the insulator section in the w plane becomes shorter and approaches the angle θ to the v direction while the fins become longer and the angle α becomes smaller. In the limit of zero b, both a and α become zero and the fins should each become $\frac{1}{2}d\tan\theta$ in length in the $-u$ direction flattened and lying against each other. This then reproduces the continuous electrode

Downloaded from rsta.royalsocietypublishing.org

problem. The current flows at an angle θ to the v axis whilst $\mathbf{E}'$ is parallel to the v axis. In the main region of the duct $\mathbf{E}'$ should also be parallel to y viewed in the z plane. It is clearer to follow a path of constant x in the w plane. Then, from the lower electrode it must, in this limit, proceed a distance $\frac{1}{2}d\tan\theta$ in the $-u$ direction to the end of the fin, then cross the duct parallel to the v axis and at the opposite electrode pass between two fins in the $-u$ direction a distance $\frac{1}{2}d\tan\theta$. Thus in the limit of zero b, $\Delta_u = -\frac{1}{2}d\tan\theta$ and $\Delta_v = 0$, which satisfies (22). For small b, α can be determined by using equation (64) in the appendix from

$$-\frac{\alpha}{\pi}\ln b = \frac{d}{4\rho}\tan\theta = -\tfrac{1}{2}\Delta_u = \frac{\text{leakage current}}{\text{electrode current}}$$

while $\Delta_v = 0$ is verified.

The condition for no shorting is essentially $a \leqslant b$. From (20) this imposes a minimum value on b depending on α, namely

$$b \geqslant \frac{2\alpha}{\frac{1}{2}\pi+\theta}. \tag{23}$$

For oppositely connected electrode pairs (22) shows that α has a maximum value of θ corresponding to $d/2\rho \to \infty$ for finite b. Therefore the necessary and sufficient condition (23) can be reduced to a sufficient condition given by Witalis,

$$\frac{\text{insulator length}}{\text{electrode length}} = \frac{b}{2-b} \geqslant \frac{2\theta}{\pi}, \tag{24}$$

or, since θ has a maximum value of $\frac{1}{2}\pi$ it is sufficient for the insulator to be the same length as the electrode as used by Hurwitz *et al.* (1961). Naturally there is least ohmic dissipation when b is made as small as is consistent with condition (23). These results can also be obtained from the next method.

Method II. Fourier analysis

In a long multisegment duct the current pattern away from the ends should repeat itself at each segment pair. Hence the method of Fourier analysis can be used. In addition, this technique allows the solution of current distribution even when non-uniformities in plasma parameters are present. However, the present paper confines its attention to uniform electrical properties and the solution of Laplace's equation. No assumptions of homogeneity in the centre of duct or smallness of segments need be made, and an exact solution can be obtained.

To take advantage of the symmetry of the current pattern, the points $x = 0$ and $y = 0$ are chosen at the centre of the duct opposite two facing electrodes as in figure 3.

A solution of Laplace's equation for ψ can be written as

$$\psi = \psi_0 + (a_0 x/\rho) + (b_0 y/\rho) + \sum_{n=1}^{\infty}[a_n \cosh(\pi n y/\rho)\sin(\pi n x/\rho) + b_n \sinh(\pi n y/\rho)\cos(\pi n x/\rho)]. \tag{25}$$

However, the boundary conditions on the electrodes give an infinite set of linear equations for a_n and b_n of the form

$$\left.\begin{aligned} a_n &= B_{mn}\, b_m, \\ b_n &= A_{mn}\, a_m + \alpha_n. \end{aligned}\right\} \tag{26}$$

Downloaded from rsta.royalsocietypublishing.org

An alternative approach was suggested by Lighthill (private communication). If we write

$$j_x + \mathrm{i}j_y = j\mathrm{e}^{\mathrm{i}\phi} \tag{27}$$

equations (12) and (14) yield a set of Cauchy–Riemann relations

$$\left.\begin{aligned} \frac{\partial \phi}{\partial x} &= \frac{\partial}{\partial y} \ln j, \\ \frac{\partial \phi}{\partial y} &= -\frac{\partial}{\partial x} \ln j, \end{aligned}\right\} \tag{28}$$

and ϕ is a solution in Laplace's equation

$$\frac{\partial^2 \phi}{\partial x^2} + \frac{\partial^2 \phi}{\partial y^2} = 0. \tag{29}$$

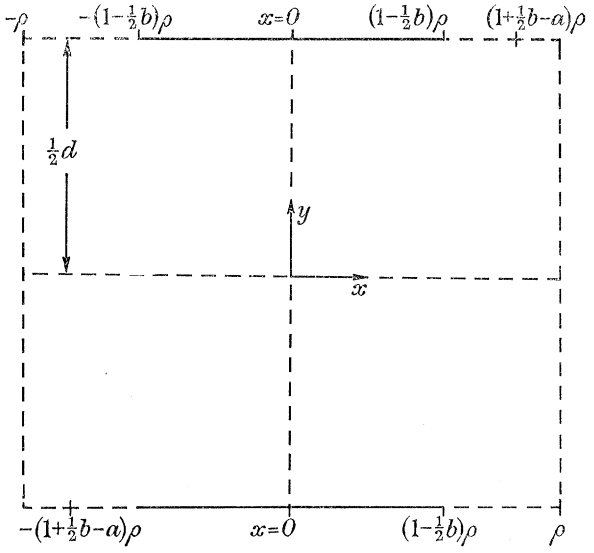

FIGURE 3. Diagram showing the x coordinate positions used in the Fourier analysis method.

The boundary conditions for ϕ are known explicitly on the insulator and electrode, except for the uncertainty of the location of the stationary points at $x = (1+\frac{1}{2}b-a)$, $y = \frac{1}{2}d$ and $x = -(1+\frac{1}{2}b-a)$, $y = -\frac{1}{2}d$. To overcome this $\phi(x, \frac{1}{2}d)$ is written as

$$\phi(x, \tfrac{1}{2}d) = \phi_1(x) + \phi_2(x), \tag{30}$$

where

$$\begin{aligned} \phi_1 &= \pi \quad (-\rho \leqslant x \leqslant -(1-\tfrac{1}{2}b)\rho) \\ &= \tfrac{3}{2}\pi + \theta \quad (-(1-\tfrac{1}{2}b)\rho \leqslant x \leqslant (1-\tfrac{1}{2}b)\rho) \\ &= 2\pi \quad ((1-\tfrac{1}{2}b)\rho \leqslant x \leqslant \rho), \end{aligned}$$

and

$$\begin{aligned} \phi_2 &= 0 \quad (-\rho \leqslant x \leqslant (1+\tfrac{1}{2}b-a)\rho) \\ &= -\pi \quad ((1+\tfrac{1}{2}b-a)\rho \leqslant x \leqslant \rho), \end{aligned}$$

or

$$\begin{aligned} \phi_1 = (\tfrac{3}{2}\pi + \theta - \tfrac{1}{2}\theta b) + \sum_n [&(2\theta/n) \sin \pi n(1-\tfrac{1}{2}b) \cos(\pi n x/\rho) \\ &+ 1/n \{\cos \pi n(1-\tfrac{1}{2}b) - \cos \pi n\} \sin(\pi n x/\rho)] \end{aligned}$$

and

$$\begin{aligned} \phi_2 = -\tfrac{1}{2}\pi(a-\tfrac{1}{2}b) + \sum_n [&(1/n) \sin \pi n(1+\tfrac{1}{2}b-a) \cos(\pi n x/\rho) \\ &+ (1/n) \{\cos \pi n - \cos \pi n(1+\tfrac{1}{2}b-a)\} \sin(\pi n x/\rho)]. \end{aligned} \tag{31}$$

Downloaded from rsta.royalsocietypublishing.org

Now the solution of (29) is of the form

$$\phi(x, y) = a_0 + \sum_n [a_n \cosh(\pi n y/\rho) \cos(\pi n x/\rho) + b_n \sinh(\pi n y/\rho) \sin(\pi n x/\rho)], \quad (32)$$

where, by symmetry,

$$\phi(x, y) = \phi(-x, -y). \quad (33)$$

Applying the boundary condition (30) and (31) we find the coefficients to be

$$a_0 = \tfrac{3}{2}\pi + \theta - \tfrac{1}{2}\theta b - \tfrac{1}{2}\pi(a - \tfrac{1}{2}b),$$

$$a_n = \frac{1}{n \cosh(\pi n d/2\rho)} \{(2\theta/\pi) \sin \pi n(1 - \tfrac{1}{2}b) + \sin \pi n(1 + \tfrac{1}{2}b - a)\},$$

$$b_n = \frac{1}{n \sinh(\pi n d/2\rho)} \{\cos \pi n(1 - \tfrac{1}{2}b) - \cos \pi n(1 + \tfrac{1}{2}b - a)\}. \quad (34)$$

The constant a is found by specifying the manner in which the electrodes are externally connected. If geometrically opposite electrodes are connected and there is no cross connexion, then there is no net current flow in the x direction at $x = \rho$, i.e.

$$0 = \int_{-\frac{1}{2}d}^{+\frac{1}{2}d} j_x(\rho, y)\, dy. \quad (35)$$

Using

$$j = j_0 \exp\{\sum_n [b_n \cosh(\pi n y/\rho) \cos(\pi n x/\rho) - a_n \sinh(\pi n y/\rho) \sin(\pi n x/\rho)]\} \quad (36)$$

from (28), condition (35) can be written

$$0 = \int_0^{\frac{1}{2}d} \exp\{\sum_n (-1)^n b_n \cosh(\pi n y/\rho)\} \cos\{a_0 + \sum_n [-1]^n a_n \cosh(\pi n y/\rho)\}\, dy, \quad (37)$$

where it is noted that midway along the insulators (at $x = \rho$)

$$j(\rho, y) = j(\rho, -y). \quad (38)$$

Equation (37) essentially determines a. For $d/2\rho \gg 1$, equation (37) indicates that $\cos a_0 = 0$, and from (34) this means $a_0 = \frac{3}{2}\pi$ and

$$a + b(\theta/\pi - \tfrac{1}{2}) - 2\theta/\pi = 0. \quad (39)$$

This is the same result as obtained by Witalis by a conformal transformation, and yields the same criterion for no shorting between adjacent segments.

The Fourier analysis method not only makes no assumption about the relative sizes of d and ρ but also is amenable to solution when the electrical properties σ and β are non uniform (but still periodic). In the notation of (27) there are now modifications to (28) and (29), namely

$$\frac{\partial}{\partial y} \ln j - \frac{\partial \phi}{\partial x} = f \cos\phi,$$

$$\frac{\partial}{\partial x} \ln j + \frac{\partial \phi}{\partial y} = -f \sin\phi,$$

and

$$\frac{\partial^2 \phi}{\partial x^2} + \frac{\partial^2 \phi}{\partial y^2} + \frac{\partial}{\partial y}(f \sin\phi) + \frac{\partial}{\partial x}(f \cos\phi) = 0,$$

where

$$f = (\cos\phi + \beta \sin\phi) \frac{\partial}{\partial y} \ln\sigma - (\sin\phi - \beta \cos\phi) \frac{\partial}{\partial x} \ln\sigma - \sin\phi \frac{\partial \beta}{\partial y} - \cos\phi \frac{\partial \beta}{\partial x}.$$

Downloaded from rsta.royalsocietypublishing.org

Method III. An approximate equivalent circuit

From the point of view of obtaining a value for the effective internal resistance and assessing the degree of shorting of adjacent segments, the plasma can approximately be replaced by an equivalent resistance network as illustrated in figure 4. Here the continuous current distribution is replaced by discrete circuit elements which broadly follow the geometric path of the current. Since $j_x = \sigma E_x$ in the plasma immediately adjacent to the

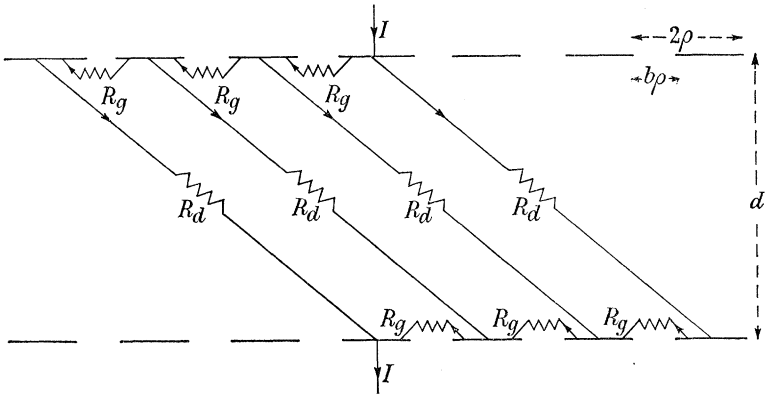

Figure 4. The approximate equivalent electric circuit for the current component flowing between one pair of oppositely connected electrodes.

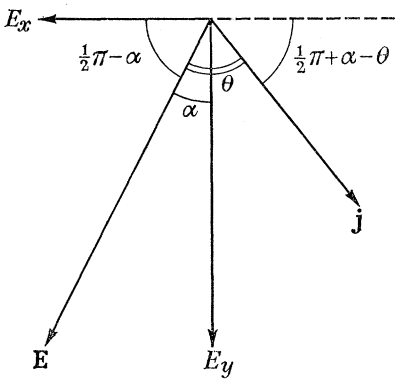

Figure 5. Orientation of the electric vector and current density vector in the central region of the duct.

insulator and since from a distance 2ρ from the wall the current flows in an almost homogeneous way—but at an angle to be determined, it was thought that this circuit could represent very closely the exact formulation of method II. Figure 4 illustrates the current paths followed by the current component of one electrode pair when the current in the channel crosses three segments. The four current paths each have the same impedance and so the current will divide equally between them. In general if the current jumps n segments as it crosses the channel, the total current in each segment gap resistance R_g due to all segments is

$$I\sum_{m=0}^{n-1}\frac{n-m}{n+1} = \tfrac{1}{2}nI, \tag{40}$$

where I is the current fed externally to each electrode. The leakage currents then exactly

Downloaded from rsta.royalsocietypublishing.org

balance the forward Hall currents in the homogeneous part of the channel. Therefore the voltage V_0 between any opposite pair of electrodes is

$$V_0 = I(\tfrac{1}{2}n^2R_g + R_d). \tag{41}$$

The quantity n is an unknown to be determined by a self consistent solution of the homogenous section of the channel. The voltage drop across adjacent segments is the same each side of the channel and so in the centre of the channel there is an electric field in the $-x$ direction of magnitude.

$$|E_x| = \frac{n}{2}\frac{IR_g}{2\rho}. \tag{42}$$

Similarly,

$$|E_y| = V_0/d. \tag{43}$$

Thus knowing the direction of the total electric field vector from these two equations, and that the current flows across the channel at an angle $\theta = \tan^{-1}\beta$ to this and at an angle $\tan^{-1}(d/2n\rho)$ to the x axis, we have, referring to figure 5, that the self consistent equation to determine n is

$$\tan(\pi/2 + \alpha - \theta) = \mathrm{d}/(2n\rho) \tag{44}$$

where

$$\tan\alpha = \frac{|E_x|}{|E_y|} = \frac{d}{2\rho}\frac{\tfrac{1}{2}nR_g}{\tfrac{1}{2}n^2R_g + R_d}. \tag{45}$$

The resistances R_g and R_d can be written approximately as

$$R_g = \left[\int_{\frac{1}{2}b\rho}^{\rho}\frac{\sigma c}{\pi r}\mathrm{d}r\right]^{-1} = \frac{\pi}{\sigma c \ln(2/b)} \tag{46}$$

and

$$R_d = \frac{1}{\sigma c \sin^2(\frac{1}{2}\pi + \alpha - \theta)}\left[\frac{d-4\rho}{2\rho} + \frac{4}{2-b}\right]. \tag{47}$$

R_d includes a correction for the convergence of the homogenous current on to electrodes $(2-b)\rho$ in length. Essentially R_d is made up of a central portion of length

$$(d-4\rho)\operatorname{cosec}(\tfrac{1}{2}\pi + \alpha - \theta)$$

and area of cross section $2\rho c \sin(\frac{1}{2}\pi + \alpha - \theta)$, and two ends, adjacent to the electrodes, each of length $2\rho\operatorname{cosec}(\frac{1}{2}\pi + \alpha - \theta)$ and area $\rho c(2-b)\sin(\frac{1}{2}\pi + \alpha - \theta)$. R_g was calculated assuming semicircular current paths between adjacent coplanar electrodes. Comparison of equations (46) and (64) shows a similar functional dependence.

Equation (44) then gives

$$\tan^{-1}\left(\frac{d}{2n\rho}\right) + \tan^{-1}\left[\frac{2n\rho}{d} + \frac{2}{n\pi}\ln(2/b)\left(1 + \frac{2\rho}{d}\frac{2b}{2-b}\right)\left(1 + \left\{\frac{2n\rho}{d}\right\}^2\right)\right] = \pi - \theta, \tag{48}$$

which determines n for given $d/2\rho$, b and θ. (It is easier to choose n and determine θ.) The ideal resistance of a segmented generator is $d/2\rho c\sigma$ and the ratio ν of actual to ideal is

$$\begin{aligned}\nu &= (\tfrac{1}{2}n^2 R_g + R_d)\frac{2\rho c\sigma}{d} \\ &= 1 + \left(\frac{2\rho}{d}\right)\frac{2b}{2-b} + n^2\left\{\left(\frac{2\rho}{d}\right)^2\left(1 + \frac{2\rho}{d}\frac{2b}{2-b}\right) + \frac{\pi\rho}{d\ln(2/b)}\right\}.\end{aligned} \tag{49}$$

In general n is not an integer, and if $n < 1$ this indicates there is no shorting. In the limit $b \to 0$ the equations give $\tan\theta = 2n\rho/d$, $R_g = 0$ and $\nu = 1 + \tan^2\theta$ correctly; and when

Downloaded from rsta.royalsocietypublishing.org

$\theta = 0$, $n = 0$. The condition for no current leakage ($n \leqslant 1$) in the limit of $d/2\rho \gg 1$ differs from the results of methods I and II and is

$$\frac{2}{\pi}\ln\frac{2}{b} \leqslant \tan\left(\tfrac{1}{2}\pi - \theta\right). \tag{50}$$

This method, while not reproducing the exact shorting condition, may be a good guide to a realistic segmented duct, because, for instance, in practice the large concentration of current density on the edge of each electrode predicted by the other methods will not occur because the electrode cannot maintain a constant potential at this edge. In addition, such effects as a higher conductivity in the region of the electrode can easily be incorporated into the model by reducing R_g.

Conclusion

An exact solution of current distribution in a segmented electrode m.h.d. duct has been found by Fourier analysis (method II). This is compared with an approximate conformal mapping procedure (method I) and an even more approximate equivalent circuit (method III), all of which illustrate the phenomenon of current leakage between adjacent segments. A sufficient condition for preventing leakage currents is given.

Appendix. The conformal transformation integral

In this section the integral in (21) is evaluated for the transformation given in (17). The result of this is quoted in one form by Witalis (1965). Writing,

$$s = \frac{\sin\frac{1}{2}\pi(z/\rho - b)}{\sin\frac{1}{2}\pi z/\rho} = \cos\tfrac{1}{2}\pi b - \cot\tfrac{1}{2}\pi\,(z/\rho)\sin\tfrac{1}{2}\pi b \tag{51}$$

and, following from this,

$$\mathrm{d}z = \frac{2\rho}{\pi}\frac{\sin\frac{1}{2}\pi b\,\mathrm{d}s}{1 - 2s\cos\frac{1}{2}\pi b + s^2}$$

the integral represented by equations (21) and (17) can be written in the s plane instead of the z plane as

$$\int_0^\infty \left(\frac{\mathrm{d}w}{\mathrm{d}z} - 1\right)_{z=1y} \mathrm{d}z = -\frac{2\rho}{\pi}\int_{s_1}^{s_2} \frac{s^{-\frac{1}{2}+\theta/\pi}\,\mathrm{e}^{-\mathrm{i}\alpha}\left[\sin\frac{1}{2}\pi\,(a-b) - s\sin\frac{1}{2}\pi a\right] + \sin\frac{1}{2}\pi b}{1 - 2s\cos\frac{1}{2}\pi b + s^2}\,\mathrm{d}s \tag{52}$$

where

$$s_1 = \cos\tfrac{1}{2}\pi b + \mathrm{i}\infty \quad \text{and} \quad s_2 = \cos\tfrac{1}{2}\pi b + \mathrm{i}\sin\tfrac{1}{2}\pi b. \tag{53}$$

The integral along $z = iy$ is now a line parallel to the imaginary s axis displaced by a distance $\cos\frac{1}{2}\pi b$. Because $\theta < \frac{1}{2}\pi$ there is a singularity in the integrand at $s = 0$, which is of no concern here, although, since it corresponds to the point $z = b\rho$ it enters into the calculation of fin length and leakage currents in the comments on this paper by Norris (p. 576 below). More important, at $s = s_2$ the denominator of the integrand is zero, but, because of equation (20) the numerator is also zero, and, on expansion, there is in fact no pole here.

Upon further investigation of the s plane the point $s = s_2$ is seen to correspond to $y = \infty$ in the z plane for *any* x. The value of x is determined by the angle at which s_2 is approached; the angle is $\pi x/\rho$ rotating anticlockwise to the vertical (imaginary) axis,

i.e.

$$\lim_{y\to\infty} \arg\,(s - s_2) = \tfrac{1}{2}\pi + \pi x/\rho. \tag{54}$$

Hence for y large, $x = 0$ is vertically above s_2, and $x = \pm\rho$ is vertically below s_2. The point $s = s_2$ can be considered as a branch point with the cut being the perpendicular from s_2 to the real axis, this latter

Downloaded from rsta.royalsocietypublishing.org

corresponding to $y = 0$, $x \neq 0$. The infinite semicircle in the upper half of the s plane corresponds to $y = 0$, $x = 0$ and the position on the semicircle gives $\mathrm{d}y/\mathrm{d}x$ at $y = 0$, $x = 0$, namely

$$\lim_{\substack{y\to 0\\ x\to 0}} \frac{\mathrm{d}y}{\mathrm{d}x} = -\lim_{s\to\infty} \tan \arg s. \tag{55}$$

In order to evaluate the integral in (52) the path of integration in the s plane is changed to the radius vector from infinity to s_2 given by $s = (1/t)\exp \tfrac{1}{2}\mathrm{i}\pi b$

where t is real and is taken from 0 to 1. This corresponds in the z plane to the path from $y = 0$, $x = 0$, $\mathrm{d}y/\mathrm{d}x = -\tan \tfrac{1}{2}\pi b$ to $y = \infty$, $x = -\tfrac{1}{2}\rho\,(1-b)$. Since $z = 0$ corresponds to $w = 0$ and since $\mathrm{d}w/\mathrm{d}z - 1 = 0$ at $y = \infty$, the integral in equation (52) is unaffected by the change in path. Then from equation (20) the numerator of the integrand in equation (52) becomes

$$\tfrac{1}{2}\mathrm{i}t^{-\frac{1}{2}-\theta/\pi}\left[\mathrm{e}^{\frac{1}{2}\mathrm{i}\pi b} - t\mathrm{e}^{-\frac{1}{2}\mathrm{i}\pi b} - (1-t)\,\mathrm{e}^{-\mathrm{i}(2\alpha-\theta b)}\right] - \tfrac{1}{2}\mathrm{i}\left[\mathrm{e}^{\frac{1}{2}\mathrm{i}\pi b} - \mathrm{e}^{-\frac{1}{2}\mathrm{i}\pi b}\right]$$

while

$$-\frac{\mathrm{d}s}{1-2s\cos\tfrac{1}{2}\pi b + s^2} = \frac{\mathrm{e}^{-\frac{1}{2}\mathrm{i}\pi b} - t\mathrm{e}^{\frac{1}{2}\mathrm{i}\pi b}}{(1-t)\,(1-2t\cos\pi b + t^2)}\,\mathrm{d}t,$$

thus giving the results of Witalis for the shifts Δ_u and Δ_v in equation (21),

$$\left.\begin{aligned} \pi\Delta_u &= I_1\sin\beta - I_2\sin\gamma + \tfrac{1}{2}\pi(1-b)\\ \pi\Delta_v &= I_1\cos\beta - I_2\cos\gamma - I_3 - \tfrac{1}{2}\ln(2-2\cos\pi b)\end{aligned}\right\} \tag{56}$$

where

$$\left.\begin{aligned} I_1 &= \int_0^1 \frac{t^{\frac{1}{2}-\theta/\pi}}{1-2t\cos\pi b + t^2}, \quad I_2 = \int_0^1 \frac{t^{-\frac{1}{2}-\theta/\pi}\,\mathrm{d}t}{1-2t\cos\pi b + t^2}\\ I_3 &= \int_0^1 \frac{1-t^{-\frac{1}{2}-\theta/\pi}}{1-t}\,\mathrm{d}t = \int_0^\infty \frac{\mathrm{e}^{-q} - \mathrm{e}^{-(\frac{1}{2}-\theta/\pi)q}}{1-\mathrm{e}^{-q}}\,\mathrm{d}q\\ &= j + \psi_1(\tfrac{1}{2}-\theta/\pi) = -\frac{1}{\frac{1}{2}-\theta/\pi} + \sum_{n=1}^{\infty}\left[\frac{1}{n} - \frac{1}{n+\frac{1}{2}-\theta/\pi}\right]\end{aligned}\right\} \tag{57}$$

j = Euler's constant = $0{\cdot}5772\ldots = -\psi_1(1)$

$$\psi_1(z) = \mathrm{d}\ln\Gamma(z)/\mathrm{d}z$$

(see, for example, Morse & Feshbach p. 422–3)

$$\left.\begin{aligned} \beta &= 2\alpha - \theta b - \tfrac{1}{2}\pi b,\\ \gamma &= 2\alpha - \theta b + \tfrac{1}{2}\pi b.\end{aligned}\right\} \tag{58}$$

Using a Taylor or Fourier expansion of the form

$$\frac{1}{1-2t\cos\pi b + t^2} = \sum_{n=1}^{\infty}\frac{\sin n\pi b}{\sin\pi b}\,t^{n-1} \tag{59}$$

the integrals I_1 and I_2 can also be represented as Fourier series

$$\left.\begin{aligned} I_1 &= \sum_{n=1}^{\infty}\frac{\sin n\pi b}{(n+\frac{1}{2}-\theta/\pi)\sin\pi b},\\ I_2 &= \sum_{n=1}^{\infty}\frac{\sin n\pi b}{(n-\frac{1}{2}-\theta/\pi)\sin\pi b}.\end{aligned}\right\} \tag{60}$$

A further alternative expansion of the integrals is useful for small b, i.e. small insulation lengths. Writing $r = 1-t$ and $\phi = \frac{1}{2}-\theta/\pi$ expansion of equation (57) yields

$$\begin{aligned} I_1(b,\phi) &= \int_0^1 \frac{1 - \phi r + \dfrac{\phi(\phi-1)}{2!}r^2 - \dfrac{\phi(\phi-1)(\phi-2)}{3!}r^3\ldots}{r^2 + 2(1-r)(1-\cos\pi b)}\,\mathrm{d}r\\ &= \tfrac{1}{2}\pi\frac{1-b}{\sin\pi b} + \tfrac{1}{2}\phi\ln(2-2\cos\pi b) + \frac{\phi(\phi-1)}{1{\cdot}2!} - \frac{\phi(\phi-1)(\phi-2)}{2{\cdot}3!}\\ &\quad + \frac{\phi(\phi-1)(\phi-2)(\phi-3)}{3{\cdot}4!} - \ldots + O(b)\end{aligned} \tag{61}$$

Downloaded from rsta.royalsocietypublishing.org

while I_2 and I_3 are simply

$$I_2(b,\phi) = \frac{1}{\phi} - I_1(b,\phi+1) + 2\cos\pi b\, I_1(b,\phi) \tag{62}$$

and

$$I_3(\phi) = -\frac{1}{\phi} + \phi - \frac{\phi(\phi-1)}{2\cdot 2!} + \frac{\phi(\phi-1)(\phi-2)}{3\cdot 3!} \ldots \tag{63}$$

Now equation (22) determines the angle α for a given b when opposite electrodes are connected in pairs. When b is very small, equation (22) is consistent with α also being small. The shifts Δ_u and Δ_v in equation (56) in the limit of small b become

$$\left.\begin{aligned} \pi\Delta_u &= (\ln\pi b + I_3)\sin 2\alpha + \tfrac{1}{2}\pi(1-\cos 2\alpha) + O(b) \\ \pi\Delta_v &= -(\ln\pi b + I_3)(1-\cos 2\alpha) + \tfrac{1}{2}\pi\sin 2\alpha + O(b). \end{aligned}\right\} \tag{64}$$

where equations (61), (62) and (63) have been employed.

References (Haines)

Crown, J. C. 1961 United Aircraft Rep. R. 1852–2.
Hurwitz, H., Kilb, R. W. & Sutton, G. W. 1961 *J. Appl. Phys.* **32**, 205.
Kemp, N. H. & Petschek, H. E. 1958 *J. Fluid Mech.* **4**, 553.
Kerrebrock, J. L. 1965 *6th Symp. on engineering aspects of m.h.d.* University of Pittsburgh.
Morse, P. M. & Feshbach, H. 1953 *Methods of theoretical physics.* New York: McGraw-Hill.
Schlüter, A. 1950 *Z. Naturf.* **5***a*, 72.
Schlüter, A. 1951 *Z. Naturf.* **6***a*, 73.
Schultz, F. & Denzel, D. C. 1964 *Int. Proc. Symp. on m.h.d. elect. power gen., Paris*, E.N.E.A. (O.E.C.D.).
Wick, R. F. 1954 *J. Appl. Phys.* **25**, 741.
Witalis, E. A. 1965 *J. Nucl. En.* C **7**, 235, 455.

Note. A further work on this subject by Dr L. S. Dzung in *Brown Boveri Rev.* **53**, 238 (1966) covers much the same ground as that by Witalis (1965).